

## Determination of the quench velocity and rewetting temperature of hot surfaces: Formulation of a nonisothermal microscale hydrodynamic model

M. Ben David,<sup>1</sup> Y. Zvirin,<sup>2</sup> and Y. Zimmels<sup>1</sup>

<sup>1</sup>*Department of Civil Engineering, Technion–Israel Institute of Technology, Haifa 32000, Israel*

<sup>2</sup>*Department of Mechanical Engineering, Technion–Israel Institute of Technology, Haifa 32000, Israel*

(Received 30 June 1998; revised manuscript received 17 February 1999)

A nonisothermal microscale model of the three-phase, solid-liquid-gas, contact zone is formulated in the context of rewetting phenomena. The model incorporates hydrodynamics, heat transfer, interfacial phenomena, and intermolecular long range forces, in a two-dimensional proximal region of the order of 1000 Å in width and 100 Å in thickness. The model comprises scaled mass, momentum, and energy balances, and their corresponding scaled boundary conditions. The small contact angles which are characteristic of rewetting situations facilitate the use of the lubrication approximation, and the dynamics of the liquid and gas phases is decoupled by applying the one-sided simplification. The microscale hydrodynamic model reflects the strong effect of the solid-liquid interactions on the film profile, and the attendant flow and thermal fields. Thinner films having smaller contact angles involve stronger solid-liquid attraction forces, and consequently they exhibit higher rewetting temperatures and lower evaporation and vapor recoil effects. Thermocapillary and evaporation and conduction effects are expressed by appropriate dimensionless numbers. A set of such numbers is defined in the context of the differential equations of the microscale model. This model covers the hydrodynamic aspect of rewetting phenomena, which are also controlled by thermodynamic and macroscale constraints. This calls for interfacing and appropriate combination between the microscale hydrodynamic model, thermodynamics, and other macroscale rewetting models, for the determination of rewetting temperatures and quench velocities of liquids on hot solid surfaces. This is addressed elsewhere, in subsequent papers that follow this work. [S1063-651X(99)00506-1]

PACS number(s): 44.35.+c, 05.70.Np, 68.10.Cr, 82.65.Dp

### I. INTRODUCTION

#### A. Problem description

Rewetting of hot surfaces is a process in which a liquid wets a hot solid surface by displacing its own vapor that otherwise prevents contact between the solid and liquid phases. When a liquid contacts a sufficiently hot surface it comes to a boiling point, and a vapor film, which separates the liquid from the surface, is generated. As the surface cools off, the vapor film reaches a point where it can no longer be sustained. At this point, the vapor film collapses and surface-liquid contact is reestablished. This phenomenon is called rewetting or quenching.

The temperature at the solid-liquid-vapor contact line, at the point where contact is reestablished, has been called by different names, such as rewetting, quenching, sputtering, or Leidenfrost temperature. Though these synonyms for the rewetting temperature do not have exactly the same physical meanings (there is much confusion regarding this point), this temperature may generally be considered as being a threshold temperature, above which liquid cannot wet the surface, or alternatively, be in contact with it.

Rewetting phenomena of hot surfaces appear in many physical processes and have important technological applications. Understanding of this phenomenon is called for in many engineering and scientific fields where it is encountered. For example, it is observed in cryogenic processes, filling of liquefied natural gas pipelines, and in high temperature metallurgy. The rewetting phenomenon is known to be of paramount importance regarding the danger of loss of coolant fluid from the cooling system of a nuclear reactor. If

such an accident occurs, the nuclear fuel rods may be exposed, with a due increase in their temperature. This rise in temperature can reach dangerous levels where melting of the rods becomes imminent. One way to avoid this situation is to flood the core of the reactor with water from top to bottom, in a process which is called “top flooding.” If the reverse direction is used, then it is called “bottom flooding.” It is therefore important to be able to predict, for these flooding processes, the velocity at which the quench front propagates, i.e., the rewetting velocity.

Several models for the rewetting velocity have been formulated in the last 30 years. Most of them require the assumption of an *a priori* value for the quench (rewetting) temperature at the three-phase, e.g., solid-liquid-vapor, contact line. There is no general method, as yet, to determine this temperature, despite several attempts that have been made, employing principles of thermodynamics, hydrodynamics, surface chemistry, and heat transfer. Using all or some of these principles still leads to predictions of different rewetting temperatures, for a specific solid-liquid system that is operated under fixed conditions.

#### B. Models based on hydrodynamic and thermodynamic theories

Reviews of rewetting models were given by Gerweck and Yadigaroglu [1], Carbajo and Siegel [2], and Ben David [3]. In the present work, reference is made to some specific models that are used at a later stage for comparison purposes. The hydrodynamic approaches include identification of heat transport mechanisms between the wall, droplets impinging

on it, and the flow boundary layer. These hydrodynamic approaches show that the heat flux attains a minimum, which depends on the flow rate, pressure, and vapor quality at a specific temperature defined as the rewetting temperature. Agreement with experimental data is limited to a few cases only. Other hydrodynamic models for rewetting temperatures are based on instability limits such as the Rayleigh-Taylor limit. A force balance indicates that the perturbation would grow when the distance between the bubbles formed on the surface reaches a critical wavelength. Models that include the above considerations were developed by Berenson [4], Henry [5], and Shoji and Takagi [6]. According to the Berenson model, the minimum film boiling (MFB) temperature for water, benzene, and ethanol, at atmospheric pressure, was found to be  $T_{\text{MFB}} = 158, 180, \text{ and } 178^\circ\text{C}$ , respectively. During rewetting, the hydrodynamic constraints must be satisfied to allow contact of the liquid with the wall, and the interface temperature must not exceed the thermodynamic limit for wetting to occur. Different values of rewetting temperatures can be expected from the different hydrodynamic approaches mentioned above. This may be due to differences in the models, or perhaps the existence of a range of the rewetting temperature, rather than a single value.

Berenson [4] was the first to present an expression for the minimum film temperature of pool boiling on a horizontal surface, that is based on the Taylor instability of the vapor-liquid interface. In his theory, the spacing of the bubbles departing from the vapor film, and their growth rate, are determined by this instability, and an analytical expression for the heat transfer coefficient near the minimum film boiling point is deduced. This heat transfer coefficient is compared with a correlation of the minimum heat flux, in order to obtain the following minimum film boiling temperature ( $T_{\text{MFB}}$ ) for a horizontal surface:

$$T_{\text{MFB}} - T_{\text{sat}} = 0.127 \frac{\rho_v H_l}{\lambda_v} \left[ \frac{g(\rho_l - \rho_v)}{\rho_l + \rho_v} \right]^{2/3} \left[ \frac{\sigma}{g(\rho_l - \rho_v)} \right]^{1/2} \times \left[ \frac{\mu_v}{g(\rho_l - \rho_v)} \right]^{1/3}, \quad (1)$$

where  $T_{\text{sat}}$ ,  $\rho$ ,  $H$ ,  $\lambda$ ,  $\sigma$ ,  $\mu$ , and  $g$  are the saturation temperature, density, heat of evaporation, thermal conductivity, liquid-vapor interfacial tension, viscosity, and gravitational acceleration, respectively. Subscripts  $l$ ,  $v$ , and  $s$  (which is used later) denote the liquid, vapor and solid phases.

The model of Berenson does not depend on the wall properties. Nevertheless, its results are in good agreement with experimental data that were obtained with several fluids. Henry [7] reported that the actual rewetting temperature values for water, freon, sodium, and potassium are significantly higher. He performed a dimensional analysis for the problem, using the infinite slab model (Carslaw and Jaeger), [8], for temperature upon contact, microlayer evaporation, and the minimum film boiling temperature from the hydrodynamic model of Berenson [Eq. (1)], and obtained the following correlation for the minimum film boiling temperature in pool boiling:

$$\frac{T_{\text{MFB}} - T_{\text{MFB},B}}{T_{\text{MFB},B} - T_l} = 0.42 \left( \zeta \frac{H_l}{c_{p,s}(T_{\text{MFB},B} - T_{\text{sat}})} \right)^{0.6}, \quad (2)$$

where  $T_{\text{MFB},B}$  is the value of  $T_{\text{MFB}}$  from the Berenson model,  $T_l$  is the liquid temperature,  $c_p$  is the heat capacity ( $c_{p,s}$  is the heat capacity of the solid), and  $\zeta$  is defined by

$$\zeta = [\lambda \rho c_p]_l / [\lambda \rho c_p]_s. \quad (3)$$

Loege, Rohsenow, and Griffith [9], developed a correlation for forced vertical flow, using water data and the Berenson correlation. Their result was given by

$$T_{\text{MFB}} - T_{\text{sat}} = (T_{\text{MFB},B} - T_{\text{sat}}) (1 - 0.295\chi^{2.45}) \times (1 + 0.279G^{0.49}), \quad (4)$$

where  $\chi$  is the exit quality and  $G$  is the mass flux, which ranges between 54.2 and 135.6 kg/m<sup>2</sup>s. De Salve and Panella, [10] suggested an expression for the rewetting temperature,  $T_{\text{rew}}$ , based on hydrodynamic-thermodynamic considerations. It includes the maximum superheat temperature of the liquid,  $T_{\text{max}}$ , which is based on the Spinodal limit, from Spiegler *et al.* [11] and the interface temperature of Baumeister and Simon [12], with a correction factor for the flow from Ref. [9]. Their expression is given by

$$T_{\text{rew}} = T_l + 0.29(T_{\text{max}} - T_l) (1 + 0.279G^{0.49}) \times [\exp(3.06 \times 10^6 \beta) \text{erfc}(1751.5\sqrt{\beta})]^{-1}, \quad (5)$$

where  $\beta = [\lambda \rho c_p]_s^{-1}$ . A rewetting model based on microscopic considerations was proposed by Wayner [13]. This model does not give a rewetting temperature, but it provides an expression for the rewetting velocity. The latter is obtained by modeling the fluid flow in the region, where the evaporating liquid film and the vapor join the solid surface. One of the parameters determining the flow characteristics is the disjoining pressure, which is the pressure drop, in a thin fluid layer, caused by the London-van der Waals forces between the substrate and the fluid. The final expression for the rewetting velocity,  $U_{\text{rew}}$ , based on the balance between this disjoining pressure, the pressure gradient due to surface tension, and the change in curvature of the liquid-vapor interface, is

$$U_{\text{rew}} = \frac{-A_d \delta^*}{\nu_l \left[ \rho_l \left( \delta - \frac{\delta_0}{3} \right) + \rho_s c_{p,s} \varepsilon_s (T_{\text{rew}} - T_{\text{sd}}) / H_l \right]}, \quad (6)$$

where  $\delta$  is the thickness of the fluid film,  $\delta^*$  its derivative with respect to the coordinate which moves with the quench front,  $\delta_0$  the film thickness at the junction between the evaporated region and the nonevaporated region,  $A_d$  a dispersion constant accounting for London-van der Waals forces,  $\nu_l$  the kinematic viscosity of the liquid,  $\varepsilon_s$  the thickness of the lamina being cooled, and  $T_{\text{sd}}$  the dry solid temperature. It is rather difficult to compare this expression with other known expressions for the rewetting velocity, because some of the parameters, such as  $A_d$  and  $\delta$ , cannot be deter-

mined with sufficient accuracy. Another disadvantage of this expression is the arbitrariness in setting the value of  $\varepsilon_s$ .

Most of the existing rewetting velocity models use data of rewetting temperature, as a necessary input condition at the triple-phase contact region. A characteristic feature of methods for estimation of  $T_{\text{rew}}$  is that they are either thermodynamic or hydrodynamic. In contrast to this traditional distinction, the approach that is developed in this work, and its subsequent parts, determines the rewetting temperature by the simultaneous combination of thermodynamic and hydrodynamic aspects of rewetting. In this context a significant advance is achieved through the microscaling of the rewetting phenomenon, and the incorporation of physical parameters of interfaces, such as contact angle and those related to intermolecular forces. This focuses the treatment onto a microscale region, adjacent to the three-phase contact line. The modeling method and its consequences are the subject of a four-part series. The first part, that is presented here, is a formulation of a non-isothermal micro-scale hydrodynamic model of the three-phase contact zone. The model is based on the conservation equations, and takes into account the above-mentioned phenomena, thermocapillary effects, and evaporation. Appropriate scaling, and the use of lubrication approximation, facilitate substantial simplifications of the governing equations, and boundary conditions. The second part [14], includes the derivation of the interface equation, its solution, and a parametric study of the film thickness behavior. In the third part [15], a microscale model for the contact angle  $\theta$  is added, based on the method of Sullivan [16,17]. By comparing  $\theta$  with the slope of the interface (using an iterative algorithm), a relation is obtained between the rewetting temperature  $T_{\text{rew}}$  and the quench velocity  $U_{\text{rew}}$ . Finally, these two parameters are uniquely determined in the fourth part [18], by combining the microscale model with a macroscale one developed in Ref. [19], which predicts  $U_{\text{rew}}$  if  $T_{\text{rew}}$  is known. The results, which are presented in the third and fourth parts [15,18], cover a wide range of solid-liquid properties.

## II. THEORY

### A. Scales of the rewetting region

In order to determine the dimensions of the investigated region, use was made of the classification made in Ref. [20]. They distinguished between four regions close to the contact line:

(1) A molecular domain of size  $a$  ( $\approx$  a few  $\text{\AA}$ ), very close to the triple line, where the continuum description breaks down.

(2) A proximal region (of length  $a/\theta_e^2$  and height  $a/\theta_e$ ), where the long-range van der Waals forces dominate ( $\theta_e$  is an equilibrium contact angle). In this region, forces due to capillary and Poiseuille friction effects are also significant.

(3) A central region, where capillary forces and Poiseuille friction are the only important factors.

(4) A distal region, where macroscopic features (gravitational forces, etc.) come into play.

In this work, the proximal region, where intermolecular forces (mainly van der Waals) and capillary effects are significant, is selected for the development of a microscale hydrodynamic model. van der Waals forces are long ranged,

and they become dominant at distances which are in the range of  $30\text{--}10^4 \text{\AA}$ . In their analysis of dynamic contact lines, de Gennes, Hua, and Levinson [20], showed that there is no clear characteristic length for this range. In this context, they suggested adopting the molecular size  $a$ , and found it to be convenient in scaling the various regions. This molecular size is of the order of few  $\text{\AA}$ . de Gennes [21] defined it by

$$a^2 = \frac{A}{6\pi\sigma}, \quad (7)$$

where  $A$  is the Hamaker constant. He assumed the liquid film to be almost flat (the contact angle being very small,  $\theta_e \ll 1$ ), so that the vertical dimension ( $Z$ , perpendicular to the solid) is very small in comparison to the lateral one ( $X$ , in the flow direction). de Gennes also showed that the long-range forces provide a natural cutoff for the singularity of the logarithm expression of the total dissipation near the contact line, at fluid thickness,  $H(X)$ , defined by

$$H(X) \cong \theta_e L, \quad L \cong a/\theta_e^2. \quad (8)$$

The lengths given in Eqs. (8) determine the region where long-range van der Waals forces prevail. This work is concerned with the range in which these forces influence the rewetting process. To this end, employing the de Gennes' classification of wetting regions facilitates the development of a microscale rewetting model.

Following de Gennes [21], the crossover length which relates to the expressions of disjoining pressure, in retarded and nonretarded situations, is about  $100 \text{\AA}$ . This means that for film thickness of  $O(100 \text{\AA})$ , the disjoining pressure, due to long-range van der Waals forces, should be included in the force balance. Therefore, the momentum balance, which is formulated in this work, includes a special term accounting for this intermolecular force. Note that this "scale check" has been made for all fluids considered in this work. The use of de Gennes' classification of wetting regions means that, in this work, the scaling lengths of the region investigated are those given by Eq. (8).

### B. Basic assumptions

The formulation of the microscale hydrodynamic model is based on the following guidelines and assumptions.

(1) The analysis is focused on the domain close to the contact line. The magnitude of this domain is of the order of  $100 \text{\AA}$  in the vertical direction (film thickness) and  $1000 \text{\AA}$  in the horizontal direction (parallel to the solid surface).

(2) The region investigated contains a thin viscous liquid film that is bounded by its vapor (gas phase), and by a rigid wall that is held at constant temperature. The justification for this assumption is given in Sec. II C 2.

(3) The liquid film is thin enough so that gravitational effects are negligible, and van der Waals attraction forces are significant. However, the film thickness still warrants a description of the liquid as a continuum, and use of related flow theories.

(4) The liquid film consists of an incompressible Newtonian fluid.

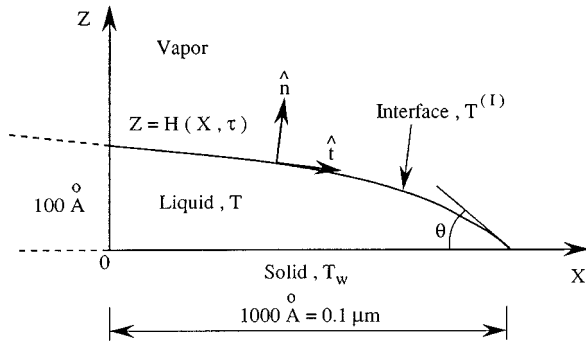


FIG. 1. Sketch of the problem geometry.

(5) The liquid properties, i.e., density, viscosity, etc., except for the surface tension, do not change significantly with temperature, and their values are taken as those under conditions of saturation temperature and atmospheric pressure.

(6) The liquid in the film evaporates. Consequently, there is heat, mass, and momentum transfer at the vapor-liquid interface. The evaporation dynamics is described by boundary condition jumps.

(7) The density, viscosity, and thermal conductivity are assumed to be considerably greater in the liquid as compared to the vapor, so that the dynamics of the vapor can be decoupled from that of the liquid.

(8) Surface phenomena such as contact angle, capillary, and thermocapillary effects are significant.

(9) The rewetting geometry is two-dimensional due to the fact that the liquid film thickness is much smaller than its longitudinal dimension.

(10) The small slopes ( $\theta \ll 1$ ), which are characteristic of the liquid-vapor interface in rewetting situations, allow the use of the lubrication approximation.

(11) The three-phase contact line moves at a nearly constant velocity,  $U_{\text{rew}}$ , so that in the moving frame of this contact line, the problem can be described as being quasi-static.

(12) When the temperature at the three-phase contact line exceeds the rewetting temperature, which is independent of time and space, no solid-liquid contact is possible.

In contrast to the currently available models, this work presents hydrodynamic modeling of film spreading that takes into account temperature and phase changes occurring along the liquid-vapor interface, as well as heat and mass transfer between the liquid and vapor phases that interact across it. This approach treats the problem in a more general way, in comparison with other known models, such as that of de Gennes [21], which deals with the isothermal case.

### C. Mathematical description of the problem

The configuration of the investigated region is shown in Fig. 1. Cartesian coordinates  $(X, Z)$  are used to describe the two-dimensional system.

The liquid-vapor interface is expressed as  $Z = H(X, \tau)$ , and the film thickness  $H$  is a function of the lateral coordinate  $X$  and time  $\tau$ . The outward normal and tangent to the interface unit vectors,  $\hat{\mathbf{n}}$  and  $\hat{\mathbf{t}}$ , are given by

$$\hat{\mathbf{n}} = (-H_X \hat{\mathbf{i}} + \hat{\mathbf{k}})(1 + H_X^2)^{-1/2}, \quad \hat{\mathbf{t}} = (\hat{\mathbf{i}} + H_X \hat{\mathbf{k}})(1 + H_X^2)^{-1/2}, \quad (9)$$

where  $\hat{\mathbf{i}}$  and  $\hat{\mathbf{k}}$  are unit vectors in the  $X$  and  $Z$  directions, respectively. The subscript  $X$  refers to a partial derivative with respect to  $X$ . This convention applies also for partial derivatives with respect to  $Z$  and  $\tau$ .

#### 1. Balance equations

The following equations express mass, momentum, and energy balances for the liquid. In the entire studied region (not including boundaries), the *mass balance* is given by the continuity equation

$$U_X + W_Z = 0, \quad (10)$$

where  $U$  and  $W$  are the velocity components in the  $X$  and  $Z$  directions. The forces acting in this region may be expressed by *momentum balances*: the horizontal direction ( $X$ ),

$$\rho_l(U_\tau + UU_X + WW_Z) = -P_X + \eta_l(U_{XX} + U_{ZZ}), \quad (11a)$$

and the vertical direction ( $Z$ ),

$$\rho_l(W_\tau + UW_X + WW_Z) = -P_Z + \eta_l(W_{XX} + W_{ZZ}), \quad (11b)$$

where  $\rho_l$  is the liquid density,  $\eta_l$  is its dynamic viscosity, and  $P$  is a generalized pressure that is defined by

$$P = P_{\text{hyd}} + \Phi. \quad (12)$$

Here  $P_{\text{hyd}}$  is the hydrodynamic pressure, and  $\Phi$  denotes a potential associated with the van der Waals attraction forces. This potential gives rise to an extra body force,  $\nabla\Phi$ , that depends on the film thickness  $H$ , cf. Ruckenstein and Jain [22]:

$$\Phi = \Phi(H) = -A/H^3 + A/Z^3. \quad (13)$$

Note that the second balance does not include the effects of  $\nabla\Phi$  nor that of gravity. There is no contribution of  $\nabla\Phi$  in the  $Z$  direction because  $\Phi$  is a function of the thickness  $H = H(X, \tau)$  only. Without loss of generality,  $P_{\text{hyd}}$  is defined as the pressure above that of the vapor,  $P_g$ , which is considered as constant.

The *energy balance* is expressed by

$$\rho_l c_{p,l}(T_\tau + UT_X + WT_Z) = \lambda_l(T_{XX} + T_{ZZ}), \quad (14)$$

where  $T$  is the temperature, which depends on time and position.

#### 2. Boundary conditions at the wall

At the solid boundary  $Z = 0$ , the no-slip condition is assumed in the  $X$  direction, the nonpenetration condition is applied in the vertical direction, and the temperature is assumed to be constant, so that

$$U = 0, \quad W = 0, \quad T = T_w \quad \text{at } Z = 0. \quad (15)$$

Note that the assumption of a constant wall temperature is justified since any possible change in temperature, due to axial heat conduction, is much smaller compared with the error entailed in rewetting temperature measurements. The order of magnitude of this possible temperature change has been estimated as follows: Owen and Pulling [23] reported that the sputtering process occurs in a range of 1–3 mm from the quench front. The initial dry-solid temperature is usually within the range of  $10^2$ – $10^3$  °C. Consequently, the average temperature gradient along the wall,  $\Delta T/\Delta X$ , is  $O(10^5$ – $10^6$  °C/m). In the new model, the scale  $L$ , which determines the horizontal length of the region considered, is  $O(1000 \text{ \AA})$ . Accordingly, an estimate for the temperature variation along the wall may be expressed by

$$\Delta T_w \cong (\Delta T/\Delta X)L, \quad (16)$$

where  $\Delta T_w$  denotes a possible wall temperature variation. Substitution of the above mentioned values into Eq. (16) shows that the temperature change,  $\Delta T_w$ , is  $O(0.01$ – $0.1$  °C), which is, indeed, less than the expected experimental error involved in measuring  $T_{\text{rew}}$ .

### 3. Boundary condition at the liquid-vapor interface

At the interface  $Z=H(X, \tau)$ , liquid-vapor jump conditions, as formulated by Delhaye [24], are applied. The liquid is assumed to evaporate in a direction normal to the liquid-vapor interface. For the sake of convenience, the mass, momentum, and energy balances are expressed through the velocity vector on both sides of the interface, i.e., in the liquid and vapor phases. On the interface there is no mass accumulation, so that the mass flux (relative to the interface)  $J$  is expressed by the following jump mass balance:

$$J = \rho_l(\mathbf{V}_l - \mathbf{V}^I) \cdot \hat{\mathbf{n}} = \rho_v(\mathbf{V}_v - \mathbf{V}^I) \cdot \hat{\mathbf{n}} \quad (17)$$

where  $\mathbf{V}_l$  and  $\mathbf{V}_v$  are the velocity vectors of the liquid and vapor, and  $\mathbf{V}^I$  is the velocity of the interface.

The *energy balance* at the interface is expressed using a similar technique. In this case, the jump energy balance takes the following form:

$$J \left\{ H_l + \frac{1}{2} [(\mathbf{V}_v - \mathbf{V}^I) \cdot \hat{\mathbf{n}}]^2 - \frac{1}{2} [(\mathbf{V}_l - \mathbf{V}^I) \cdot \hat{\mathbf{n}}]^2 \right\} + \lambda_l \nabla T \cdot \hat{\mathbf{n}} - \lambda_v \nabla T_v \cdot \hat{\mathbf{n}} + 2 \eta_l (\tilde{\boldsymbol{\tau}}_l \cdot \hat{\mathbf{n}}) \cdot (\mathbf{V}_l - \mathbf{V}^I) - 2 \eta_v (\tilde{\boldsymbol{\tau}}_v \cdot \hat{\mathbf{n}}) \cdot (\mathbf{V}_v - \mathbf{V}^I) = 0, \quad (18)$$

where  $\tilde{\boldsymbol{\tau}}_l$  and  $\tilde{\boldsymbol{\tau}}_v$  are the rate of deformation tensors in the liquid and vapor, and  $T_v$  is the vapor temperature.

The first term of Eq. (18) expresses the energy change due to the evaporation process at the interface. It accounts for the heat of evaporation and the kinetic energy differences across the interface. The second term represents the energy change occurring due to the conduction of heat across the interface. The third and fourth terms represent the energy change due to dissipating shear forces in the liquid and vapor phases.

The *normal-stress* boundary condition (jump momentum balance) is given by

$$J(\mathbf{V}_l - \mathbf{V}_v) \cdot \hat{\mathbf{n}} - (\tilde{\mathbf{T}}_l - \tilde{\mathbf{T}}_v) \cdot \hat{\mathbf{n}} \cdot \hat{\mathbf{n}} - 2B\sigma(T) = 0. \quad (19)$$

The first term of Eq. (19) stands for a component of momentum which arises due to the mass flux across the interface. The second term is the normal component of the momentum which is due to the jump in the normal stress tensors between the two phases. Here  $\tilde{\mathbf{T}}_l$  and  $\tilde{\mathbf{T}}_v$  are the stress tensors of the liquid and vapor, respectively. The forces acting normally to the interface are balanced by the capillary force. The latter is defined by the surface tension  $\sigma$  times twice the mean curvature  $B$  of the interface, which is given by

$$2B = \nabla \cdot \hat{\mathbf{n}}. \quad (20)$$

The velocities both in vapor and liquid are assumed to be slow enough so that they can be treated as incompressible fluids. The stress tensor in the liquid is given as

$$\tilde{\mathbf{T}}_l = -P\tilde{\mathbf{I}} + 2\eta_l\tilde{\boldsymbol{\tau}}_l, \quad (21)$$

where  $\tilde{\mathbf{I}}$  is the identity tensor. A similar form can be used for the vapor stress tensor, and the vapor pressure  $P_v$  may be set as a reference level, i.e., the ambient pressure.

The balance of forces tangent to the interface, constitutes the following *shear stress boundary condition*:

$$J(\mathbf{V}_l - \mathbf{V}_v) \cdot \hat{\mathbf{t}} - (\tilde{\mathbf{T}}_l - \tilde{\mathbf{T}}_v) \cdot \hat{\mathbf{n}} \cdot \hat{\mathbf{t}} + \nabla \sigma \cdot \hat{\mathbf{t}} = 0. \quad (22)$$

The jump in shear stress, is balanced by the gradient of the surface tension. The change of the surface tension along the interface, owing to its dependence on the temperature, gives rise to thermocapillary effects that are included in this boundary condition.

The surface tension is represented by a linear equation of state as follows:

$$\sigma(T) = \sigma_s - \gamma(T^I - T_s), \quad (23)$$

where  $\sigma_s$  is the surface tension at the reference saturation temperature  $T_s$  and at the given system pressure. For nearly all common liquids,  $\gamma$  is positive, so that increase of temperature leads to a decrease of the surface tension. Note that  $\gamma$  is assumed to be practically a constant, so that its derivatives, with respect to  $X$  and  $Z$  in Eq. (22), are negligible in comparison to those of the temperature.

The mass flux  $J$  is expressed by the following linearized constitutive equation, that is derived from the kinetic theory (cf. Palmer [25])

$$J = \left( \frac{\alpha \rho_v H_l}{T_s^{3/2}} \right) \left( \frac{M}{2\pi R_g} \right)^{1/2} (T^I - T_s). \quad (24)$$

It depends on the local interface temperature  $T^I$ , the molecular weight  $M$ , the universal gas constant  $R_g$ , and the dimensionless accommodation coefficient,  $\alpha$  (whose value is close to 1 for most commonly used liquids).

#### 4. One-sided model simplification

The boundary conditions at the liquid-vapor interface, i.e., Eqs. (17)–(19) and (22), describe mass, energy and force balances between the liquid and vapor. In other words, the liquid behavior is conjugate to that of the vapor. However, the values of thermophysical properties such as density, viscosity, and thermal conductivity are by far larger in the liquid as compared to those in the vapor. Therefore, following our basic assumption [No. (7) in Sec. II B], the balance equations are simplified, e.g., according to Burelbach, Bankoff, and Davis [26]. As an example, only the energy boundary condition [Eq. (18)] is derived here in detail. As the same simplifications have been applied to the other boundary conditions at the interface [see Eqs. (19) and (22)], only their final forms are presented below.

The energy balance equation (18) is transformed into a simpler form by applying several algebraic steps. The velocity differences are expressed in terms of the mass flux and density by substitution of the jump mass balance from Eq. (17). Assuming that  $\nabla T_v \cdot \hat{\mathbf{n}}$ ,  $\tilde{\boldsymbol{\tau}}_l \cdot \hat{\mathbf{n}}$ , and  $\tilde{\boldsymbol{\tau}}_v \cdot \hat{\mathbf{n}}$  are all bounded, and rearranging the terms, gives

$$J \left\{ H_l + \frac{1}{2} \left( \frac{J}{\rho_v} \right)^2 - \frac{1}{2} \left( \frac{J}{\rho_l} \right)^2 \right\} + \lambda_l \left\{ \nabla T \cdot \hat{\mathbf{n}} - \frac{\lambda_v}{\lambda_l} \nabla T_v \cdot \hat{\mathbf{n}} \right\} + 2 \eta_l \left( \frac{\rho_v}{\rho_l} \right) (\tilde{\boldsymbol{\tau}}_l \cdot \hat{\mathbf{n}}) \cdot \left( \frac{\mathbf{J}}{\rho_v} \right) - 2 \left( \frac{\eta_v}{\eta_l} \right) (\tilde{\boldsymbol{\tau}}_v \cdot \hat{\mathbf{n}}) \cdot \left( \frac{\mathbf{J}}{\rho_v} \right) \eta_l = 0. \quad (25)$$

By applying the limits such as  $\lambda_v/\lambda_l \rightarrow 0$ , this equation is reduced to

$$J \left\{ H_l + \frac{1}{2} \left[ \frac{J}{\rho_v} \right]^2 \right\} = -\lambda_l \nabla T \cdot \hat{\mathbf{n}}. \quad (26)$$

Equation (26) states that the heat conducted across the film is used to vaporize the liquid and supply kinetic energy to the vaporized molecules.

For the normal-stress balance, equation (19), the simplified form of the boundary condition is obtained as

$$-\frac{J^2}{\rho_v} - \tilde{\mathbf{T}} \cdot \hat{\mathbf{n}} \cdot \hat{\mathbf{n}} = 2B \sigma(T), \quad (27)$$

where the term proportional to  $J^2$  is due to the jump in densities across the interface. Since the mass balance across the interface should be conserved, the jump in densities is translated to a jump in velocities. This jump creates the force that pushes the liquid down toward the solid. Burelbach, Bankoff, and Davis [26], termed this phenomenon ‘‘vapor recoil,’’ which may cause the film to rupture.

For the shear-stress balance equation (22), using the no-slip boundary between the two viscous fluids gives

$$(\mathbf{V}_l - \mathbf{V}_v) \cdot \hat{\mathbf{t}} = 0, \quad (28)$$

and, applying the above assumption, i.e., regarding the jump in velocities, a simpler form is obtained:

$$\tilde{\mathbf{T}} \cdot \hat{\mathbf{n}} \cdot \hat{\mathbf{t}} = \nabla \sigma(T) \cdot \hat{\mathbf{t}}. \quad (29)$$

Thus the dynamics of the vapor is decoupled from that of the liquid. This results in the ‘‘one-sided model’’; see Ref. [27]. Note that the mass balance equation (10), and the linearized constitutive equation (24) remain unchanged.

The boundary conditions at the interface are presented in their general form. In the following, they are described more explicitly, i.e., the tensor  $\tilde{\mathbf{T}}$  and terms such as  $\nabla \sigma(T) \cdot \hat{\mathbf{t}}$  and  $\nabla \sigma(T) \cdot \hat{\mathbf{n}}$  are each presented in a more detailed form.

#### 5. Normal and shear stress boundary conditions: Explicit forms

Equation (27) includes terms such as  $\tilde{\mathbf{T}} \cdot \hat{\mathbf{n}} \cdot \hat{\mathbf{n}}$ , and the curvature  $2B$  of the two-dimensional interface  $Z = H(X, \tau)$ . Substitution of the expression for the normal unit vector,  $\hat{\mathbf{n}}$  [Eq. (9)] in Eq. (20) gives

$$2B = -\frac{H_{XX}}{(1 + H_X^2)^{3/2}}. \quad (30)$$

The explicit form of the stress tensor component [Eq. (21)] for a Newtonian liquid in a film with thickness  $H$ , is

$$\tilde{\mathbf{T}} \cdot \hat{\mathbf{n}} \cdot \hat{\mathbf{n}} = -P + \frac{2 \eta_l [U_X (1 - H_X^2) + (U_Z + W_X) H_X]}{(1 + H_X^2)^{1/2}}. \quad (31)$$

In the model which is developed here, the interface is limited to small slopes ( $\theta \cong H_X \ll 1$ ). The final form of the normal-stress boundary condition is obtained by substitution of a linearized form of Eqs. (30) and (31) into Eq. (27), as follows:

$$-\frac{J^2}{\rho_v} + P + 2 \eta_l [U_X + (U_Z + W_X) H_X] = -\sigma(T) H_{XX}. \quad (32)$$

The shear-stress boundary condition of Eq. (29) is considered next. The stress tensor component  $\tilde{\mathbf{T}} \cdot \hat{\mathbf{n}} \cdot \hat{\mathbf{t}}$  is written at the interface, in terms of  $Z = H(X, \tau)$ :

$$\tilde{\mathbf{T}} \cdot \hat{\mathbf{n}} \cdot \hat{\mathbf{t}} = \frac{\eta_l [(U_Z + W_X)(1 - H_X^2) - 4U_X H_X]}{(1 + H_X^2)^{1/2}}. \quad (33)$$

Upon using the expression for the surface tension, [Eq. (23)], and that of the tangent unit vector  $\hat{\mathbf{t}}$  [Eq. (9)], the explicit result for the second term in Eq. (29) is obtained as

$$\nabla \sigma(T) \cdot \hat{\mathbf{t}} = -\frac{\gamma(T_X + T_Z H_X)}{(1 + H_X^2)^{1/2}}. \quad (34)$$

Substitution of expressions (33) and (34) into Eq. (29), and using the assumption  $H_X \ll 1$ , gives the shear stress balance in the following form:

$$\eta_l (U_Z + W_X - 4U_X H_X) = -\gamma(T_X + T_Z H_X). \quad (35)$$

**6. Kinematic boundary condition: Explicit form**

The jump mass balance specified in Eq. (17) leads to the kinematic condition at the interface, where a particle moves with the velocity  $\mathbf{V}^I$ . The modulus of  $\mathbf{V}^I$  is the same as that of the interface velocity,  $dH/d\tau$ . The boundary condition for the mass balance involves mass transport across the interface, with the following flux:

$$J = \rho_l(\mathbf{V}_l - \mathbf{V}^I) \cdot \hat{\mathbf{n}} = \frac{\rho_l(H_\tau - UH_X + W)}{(1 + H_X^2)^{1/2}}. \tag{36}$$

The small slope assumption leads to the following simplified form for the kinematic boundary condition:

$$J = \rho_l(-H_\tau - UH_X + W). \tag{37}$$

At this stage, we have a system of four partial differential equations (10), (11), and (14): mass, forces, and energy; four boundary conditions representing balances at the interface [Eqs. (17)–(19) and (22)]: mass, shear stress, normal stress, and energy balances; and three boundary conditions at the solid surface [Eq. (15)], specifying a no-penetration boundary, a no-slip boundary, and a fixed wall temperature. In Sec. IID, the model is further simplified, by using the lubrication approximation and an appropriate scaling, so as to facilitate analytical solution of its equations.

**D. Scaling of variables**

The small slope of the liquid-vapor interface ( $H_X \ll 1$ ) allows the adoption of the well-known lubrication approximation. The contact angle  $\theta$  is derived as  $H_X$  and rescaled through a reference contact angle  $\theta_o$ . Its value is very small ( $\theta_o \ll 1$ ), and, for convenience, it can be selected to be equal to  $\theta_e$  [see Eq. (8)]. All the variables in the balance equations, that are functions of  $\theta$  are introduced by their asymptotic expansions, i.e., as a function of  $\theta_o$ . Following the scaling step, the leading-order terms in the equations, as  $\theta_o \rightarrow 0$ , constitute the ‘‘lubrication approximation.’’

The space variables ( $X, Z$ ) are scaled according to the de Gennes [21] methodology. He argued that for microscopic films, which spread with a moving contact line, there is no characteristic length. Therefore, the molecular size  $a$  is a convenient choice for rescaling, and the lengths in the  $X$  and  $Z$  directions are scaled by the dimensions given in Eq. (8). The time scale is constructed by combining the length scale  $a$  with an estimate of the average velocity of the contact line,  $U_o$ . This velocity relates to the contact angle through  $U_o \cong K\theta_o^m$ , where  $K$  and  $m$  are constants; see Ehrhard and Davis, [28] and de Gennes, Hua, and Levinson [20]. The scaling considerations applied here are similar to those of Ehrhard and Davis [28] and Burelbach, Bankoff, and Davis, [26].

Conservation of mass determines the velocity scales. The pressure scale is obtained by balancing the pressure gradients and viscous terms, which is common practice in lubrication flows. Note that the generalized pressure  $P$  includes the van der Waals intermolecular forces through the potential function  $\Phi$  [Eq. (12)]. The temperature scaling is chosen so as to

allow the largest possible dimensionless (unit order) temperature difference.

In the following, the various variables of the balance equations are scaled according to these considerations. In this way, a new workable set of dimensionless variables, that characterizes the rewetting problem in microscales, is obtained.

**1. Length scales**

The space variable  $X$  varies in the range  $0 \leq X \leq L$ . Because of the small slope,  $\theta_o \ll 1$ , the expected height of the interface is of the order of  $L\theta_o$ ; therefore, the space variable  $Z$  is scaled using this length. The dimensionless lengths  $x$  and  $z$  are thus defined by

$$x = \frac{X}{L}, \quad z = \frac{Z}{L\theta_o}, \tag{38}$$

where  $L = a/\theta_o^2$  as in Eq. (8), and  $\theta_o$  is the contact angle which, in rewetting situations, is typically very small (for example,  $\theta_o \approx 1^0$ ). Note that  $\theta_o$  is defined arbitrarily as a scaling equilibrium contact angle.

**2. Time scale**

According to de Gennes [21] and de Gennes, Hua, and Levinson, [20], very thin films that spread on a solid surface advance with an average velocity  $U_o \cong K\theta_o^m$ , where  $m \geq 1$  and  $K > 0$  are empirical constants, and  $\theta_o \geq 0$  is the dynamic contact angle. Note that this constitutive relation was proved theoretically by de Gennes [21]. The power of  $m = 3$  is suggested by data of Hoffman [29] and Tanner [30]. The coefficient  $K$  is of the order of  $10^3$  (m/sec). The time scale  $\tau$  is expressed as the ratio of the horizontal domain length  $L$  and the average contact line velocity  $U_o$ :

$$\tau = \frac{L}{K\theta_o^m}. \tag{39}$$

**3. Velocity scale**

According to these time and length scales, the velocity scales are determined by the conservation of mass. The horizontal velocity  $U$  is scaled by the average contact line velocity, so that  $u = U/U_o$ . The continuity equation in dimensionless form is given by

$$\frac{\partial u}{\partial x} + \frac{\partial w}{\partial z} = 0. \tag{40}$$

This facilitates scaling of the velocity component  $w$  as

$$w = \frac{W}{K\theta_o^{m+1}}. \tag{41}$$

The dimensionless form of the continuity equation (40) is obviously the same as that of the dimensional one [Eq. (10)].

4. Pressure scale

The pressure scale is obtained through the following balance of pressure and viscous forces:

$$\eta_l U_{ZZ} = \frac{\partial P}{\partial X}. \tag{42}$$

Rescaling this balance gives

$$\frac{\partial^2 u}{\partial z^2} = \frac{\partial p}{\partial x}, \tag{43}$$

where the pressure  $p$  has the following form:

$$p = \left( \frac{L \theta_o^{2-m}}{\eta_l K} \right) P. \tag{44}$$

Similarly, rescaling of the potential function  $\Phi$  (due to van der Waals forces) yields

$$\phi = \left( \frac{L \theta_o^{2-m}}{\eta_l K} \right) \Phi. \tag{45}$$

In order to preserve the form of Eq. (13), a dimensionless potential function  $\phi$  is defined by

$$\phi = \frac{\bar{A}}{h^3}, \quad \bar{A} = (6 \pi \eta_l K L^2 \theta_o^{m+1})^{-1} A, \tag{46}$$

$$h = H / L \theta_o, \tag{47}$$

where  $h$  and  $\bar{A}$  are the dimensionless film thickness (height of the interface) and Hamaker constant, respectively. According to Eq. (12), the dimensionless pressure is then expressed by

$$p = p_{\text{hyd}} + \phi = p_{\text{hyd}} - \bar{A}/h^3 + \bar{A}/z^3. \tag{48}$$

5. Temperature scale

The temperature field is scaled through

$$\Theta = \frac{T - T_s}{T_w - T_s}. \tag{49}$$

The maximum temperature difference for the problem under consideration is  $\Delta T = T_w - T_s$ , so that  $\Theta' \leq \Theta \leq 1$ , where  $\Theta$  and  $\Theta'$  are the scaled temperature, below and at the surface, respectively.

A summary of the dimensionless (scaled) variables that characterize the rewetting problem is given as follows:

$$x = \frac{X}{L}, \quad z = \frac{Z}{L \theta_o}, \quad t = \frac{K \theta_o^m}{L} \tau,$$

$$u = \frac{U}{K \theta_o^m}, \quad w = \frac{W}{K \theta_o^{m+1}}, \quad p = \frac{L \theta_o^{2-m}}{\eta_l K} P, \quad \phi = \frac{L \theta_o^{2-m}}{\eta_l K} \Phi, \tag{50}$$

$$\Theta = \frac{T - T_s}{T_w - T_s}, \quad h = \frac{H}{L \theta_o}, \quad \bar{A} = \frac{A}{6 \pi \eta_l K L^2 \theta_o^{m+1}}.$$

The variables summarized in Eq. (50) are used, in this work, to formulate the dimensionless balance equations and boundary conditions of the new microscale hydrodynamic model.

E. Scaling of balance equations and lubrication approximation

In this section, the equations of momentum and energy balance are rewritten in terms of the dimensionless variables of Eq. (50). For the sake of brevity, only the treatment of the horizontal  $x$  component of the momentum balance is shown in detail, whereas the other equations are given only in their final form.

The dimensionless mass balance is given by the continuity equation (40). Next the momentum balance (or alternatively force balance) in the  $X$  direction, [Eq. (11a)] is transformed into a dimensionless form. Substitution of the complete set of relevant parameters from Eq. (50) into this equation gives

$$\begin{aligned} \rho_l \frac{K^2 \theta_o^{2m}}{L} \left[ \frac{\partial u}{\partial t} + u \frac{\partial u}{\partial x} + w \frac{\partial u}{\partial z} \right] \\ = - \frac{\eta_l K}{L^2 \theta_o^{2-m}} \frac{\partial p}{\partial x} + \frac{\eta_l K \theta_o^m}{L^2} \left[ \frac{\partial^2 u}{\partial x^2} + \frac{1}{\theta_o^2} \frac{\partial^2 u}{\partial z^2} \right]. \end{aligned} \tag{51}$$

Following the multiplication of Eq. (51) by the factor  $\theta_o^{2-m}$ , it turns out that the terms on the left-hand side are much smaller than those on the right-hand side. Furthermore, the second order derivative of the velocity,  $u$ , with respect to  $x$ , on the right-hand side of Eq. (51), is negligible. The result is that for  $\theta_o \rightarrow 0$ , Eq. (51) reduces to a form that is dictated by the leading order terms as follows:

$$- \frac{\partial p}{\partial x} + \frac{\partial^2 u}{\partial z^2} = 0. \tag{52}$$

Equation (52) implies that the pressure and the intermolecular interaction forces, which are represented through  $p_x$ , are balanced with the viscous forces. Note that  $\phi_x$  is part of  $p_x$ ; see Eq. 12. This form of the momentum equation is a result of what is known as the ‘‘lubrication approximation.’’

Application of the same procedure to the momentum balance in the  $z$  direction [Eq. (11b)] gives

$$\begin{aligned} \rho_l \theta_o^{m+4} \left[ \frac{\partial w}{\partial t} + u \frac{\partial w}{\partial x} + w \frac{\partial w}{\partial z} \right] \\ = - \frac{\eta_l}{LK} \left[ \frac{\partial p}{\partial z} + \theta_o^4 \frac{\partial^2 w}{\partial x^2} + \theta_o^2 \frac{\partial^2 w}{\partial x^2} \right]. \end{aligned} \tag{53}$$

An order of magnitude analysis of the last equation shows that the pressure gradient must be  $O(\theta_o^2)$  for  $m \geq 1$ , and therefore, when  $\theta_o \rightarrow 0$ , it also tends to zero. Hence, at the limit

$$\frac{\partial p}{\partial z} = 0. \tag{54}$$

The energy balance equation (14) is treated in the same way, and the result is

$$\rho_l c_{p,l} K \theta_o^{m+4} \left[ \frac{\partial \Theta}{\partial t} + u \frac{\partial \Theta}{\partial x} + w \frac{\partial \Theta}{\partial z} \right] = \frac{\lambda_l}{L} \left[ \theta_o^2 \frac{\partial^2 \Theta}{\partial x^2} + \frac{\partial^2 \Theta}{\partial z^2} \right]. \quad (55)$$

When  $\theta_o \rightarrow 0$ , this equation is reduced to

$$\frac{\partial^2 \Theta}{\partial z^2} = 0. \quad (56)$$

This form of the energy equation means that for  $\theta_o \rightarrow 0$ , the dominant mechanism of heat transport is by conduction, with subsequent superheating of the liquid and evaporation across the interface.

In summary, a substantial simplification of the balance equations is achieved by applying the lubrication approximation. Effects such as time dependence, nonlinear convection terms, and the coupling of the thermal and hydrodynamic

fields were all eliminated. In Sec. IIF, the same scaling procedure is applied to the boundary conditions at the solid wall,  $z=0$ , and at the interface,  $z=h(x,t)$ .

## F. Scaling of boundary conditions

At the solid surface, the dimensionless form of the velocity and temperature boundary conditions, [Eq. (15)] are as follows:

$$u=0, \quad w=0, \quad \Theta=1 \quad \text{at } z=0. \quad (57)$$

At the interface, which is represented in dimensionless form by  $z=h(x,t)$ , there are four boundary conditions that are scaled in the following.

### 1. Scaling of normal-stress balance

The scaling of Eq. (32) using the dimensionless variables of Eq. (50) gives

$$-\frac{L}{\theta_o} \frac{J^2}{\rho_v} + \left\{ \frac{\eta_l K}{\theta_o^{3-m}} p + 2 \eta_l K \theta_o^{m-1} \left[ \frac{\partial u}{\partial x} + \left( \frac{\partial u}{\partial z} + \theta_o^2 \frac{\partial w}{\partial x} \right) \frac{\partial h}{\partial x} \right] \right\} = -\frac{\partial^2 h}{\partial x^2} \sigma(\Theta). \quad (58)$$

The terms of Eq. (58) include different powers of  $\theta_o$ . The leading order terms of the asymptotic equation, which prevails as  $\theta_o \rightarrow 0$ , yield the following reduced form:

$$-\frac{L}{\theta_o} \frac{J^2}{\rho_v} + \frac{\eta_l K}{\theta_o^{3-m}} p = -\frac{\partial^2 h}{\partial x^2} \sigma(\Theta). \quad (59)$$

This relationship includes the mass flux  $J$  and the surface tension  $\sigma(\Theta)$ , that will now be scaled and then expressed in a dimensionless form. The former is scaled through a reference mass flux,  $J_o$ , which is due to the vaporization process that occurs at the interface.  $J_o$  is defined using a film, of reference thickness  $L\theta_o$ , that evaporates due to heat conduction which is driven by a temperature difference  $\Delta T = T_w - T_s$ .

The heat flux

$$q_o = \frac{\lambda_l \Delta T}{L \theta_o} \quad (60)$$

relates these two processes by the following simple energy balance:

$$q_o = J_o H_l = \frac{\lambda_l \Delta T}{L \theta_o}. \quad (61)$$

Thus the dimensionless mass flux  $j$  is obtained as

$$j = \frac{J}{J_o} = \frac{J H_l}{q_o} = \frac{L \theta_o H_l}{\lambda_l \Delta T} J. \quad (62)$$

Accordingly, the constitutive expression (24) for  $J$  is also expressed in a dimensionless form by inserting the expression of the nondimensional interface temperature  $\Theta^I$  and dividing by  $J_o$ ,

$$j = N \Theta^I, \quad (63)$$

where the dimensionless coefficient  $N$  is given by

$$N = \left[ \frac{L \theta_o \alpha \rho_v H_l^2}{\lambda_l T_s^{3/2}} \right] \left[ \frac{M}{2 \pi R_g} \right]^{1/2}. \quad (64)$$

The surface tension,  $\sigma(T)$  [Eq. (23)] is expressed as a function of the dimensionless temperature,  $\Theta^I$ :

$$\sigma(\Theta) = \sigma_s (1 - F \Theta^I), \quad (65)$$

where  $F$  is the capillary change factor:

$$F = \frac{\gamma \Delta T}{\sigma_s}. \quad (66)$$

Introduction of the expressions for the surface tension  $\sigma(\Theta)$  [Eq. (65)] and the dimensionless mass flux  $j$  [Eq. (63)], in conjunction with Eqs. (60) and (62), into Eq. (59), yields the following dimensionless expression for the normal stress balance:

$$-S j^2 + C p = -\frac{\partial^2 h}{\partial x^2} (1 - F \Theta^I), \quad (67)$$

where the dimensionless variables  $S$  and  $C$  are given by

$$S = \left( \frac{\lambda_l \Delta T}{L \theta_o H_l} \right)^2 \left( \frac{L}{\sigma_s \rho_v \theta_o} \right), \quad (68)$$

$$C = \frac{\eta_l K}{\sigma_s \theta_o^{3-m}} = \frac{\eta_l U_o}{\sigma_s \theta_o^3}. \quad (69)$$

It is noted that when there is no temperature gradient (isothermal case),  $S$  and  $F$  vanish, so that the Young-Laplace term prevails at the liquid-vapor interface.

The dimensionless number  $S$  [see Eq. (68)] describes the effect of kinetic energy of liquid particles that vaporize through the interface. Mass conservation, and the steep gradient of density across the interface, impose a steep gradient of velocity. At the interface, vapor particles are much faster than those of the liquid. Consequently, the interface is ‘‘pushed back,’’ and this produces a reverse reaction force that may drive the interface to exhibit significant perturbations. This effect was termed ‘‘vapor recoil’’ by Burelbach, Bankoff, and Davis [26]. The term in the first parentheses of Eq. (68) expresses the ratio between the heat transmitted by conduction and that by evaporation. The dimensionless group  $S$  expresses the evaporation process through the interface, subject to the normal stress boundary condition. The pressure term of Eq. (67) is multiplied by the dimensionless capillary number  $C$ , which is defined as the ratio of the viscous effects and surface tension effects of the moving contact line.

The term on the right-hand side of Eq. (67) is the linearized curvature multiplied by the factor accounting for variation of the surface tension with temperature. The existence of a temperature gradient along the interface produces a corresponding gradient of surface tension.

### 2. Scaling of shear stress

The result of rescaling the shear stress balance [Eq. (35)] with the variables from Eq. (50), letting  $\theta_o \rightarrow 0$ , and selecting only leading order terms, gives

$$\frac{C \theta_o^2}{F} \frac{\partial u}{\partial z} = - \left( \frac{\partial \Theta}{\partial x} + \frac{\partial \Theta}{\partial z} \frac{\partial h}{\partial x} \right) \quad \text{at } z=h. \quad (70)$$

The dimensionless number  $C/F$  expresses the thermocapillary effect. In this context, a variable surface tension is expected to develop concurrent with the occurrence of a temperature gradient along the interface. At larger distances from the three-phase contact line, the decrease in temperature produces an increase in the surface tension. The temperature induced gradient of surface tension acts to ‘‘pull’’ the advancing fluid backward (i.e., opposite to the film velocity  $U$ ). This hinders the film movement. The group  $C/F$  describes the ratio between the viscosity effects and the fractional thermal change in the surface tension. Note that, for isothermal fields, the right-hand side of Eq. (70) vanishes, and the dimensionless shear stress boundary condition is reduced to  $u_z = 0$  (the vapor seems to be passive).

### 3. Scaling of energy balance

Rescaling the energy balance of Eq. (26) in the same way, i.e., using the rescaled mass flux  $j$  through the constitutive relation (63), letting  $\theta_o \rightarrow 0$ , and leaving only the leading order terms, give

$$N \Theta^l [1 + G(N \Theta^l)^2] + \left( \frac{\partial \Theta}{\partial z} \right)_{z=h} = 0, \quad (71)$$

where the dimensionless group  $G$  is defined by

$$G = \frac{1}{2H_l^3} \left( \frac{\gamma \Delta T}{\rho_v L \theta_o} \right)^2. \quad (72)$$

The first term of Eq. (71) represents the heat consumed by evaporation, the second term refers to the kinetic energy of the vapor particles, and these two terms are balanced with the heat conducted across the film. This form of boundary condition is nonlinear in the temperature,  $\Theta^l$ . Comparison of the order of magnitude of these three energy components shows that the kinetic energy term is small relative to the evaporation term, so that Eq. (71) may be linearized. Consider, for example, the group  $e = G(N \Theta^l)^2$  for the case of water. The dimensionless numbers  $G$  and  $N$  are found to be  $O(10^{-1})$ . The dimensionless interface temperature varies between zero and one, so that  $\Theta^l \leq 1$ . It follows, then, that  $e \cong O(10^{-3})$  can be neglected with respect to 1. For further details, see Burelbach, Bankoff, and Davis, [26]. The result of neglecting the kinetic energy term in Eq. (71) yield:

$$N \Theta^l + \left( \frac{\partial \Theta}{\partial z} \right)_{z=h} = 0. \quad (73)$$

The latter boundary condition implies that the energy balance at the interface is dominated by conductive heat transfer and evaporation.

### 4. Scaling of mass balance (the kinematic condition)

Rescaling of the mass balance [Eq. (37)], and using the lubrication approximation, gives the following dimensionless kinematic boundary condition:

$$E j = w - \frac{\partial h}{\partial t} - u \frac{\partial h}{\partial x}, \quad (74)$$

where the dimensionless group  $E$  is defined by

$$E = \left( \frac{\lambda_l \Delta T}{\rho_l H_l L U_o \theta_o^2} \right). \quad (75)$$

$E$  describes a ratio of heat flow by conduction and evaporation. Expressing  $j$  in Eq. (74) by its constitutive relation [Eq. (63)] gives

$$EN \Theta^l = w - \frac{\partial h}{\partial t} - u \frac{\partial h}{\partial x}. \quad (76)$$

TABLE I. System of simplified dimensionless equations for the rewetting problem.

Mass balance—continuity		$u_x + w_z = 0$
Momentum—in the $x$ direction		$u_{zz} = p_x$
Momentum—in the $z$ direction		$p_z = 0$
Energy balance		$\Theta_{zz} = 0$
Liquid-solid potential of interaction		$\phi = \bar{A}/h^3$ (included in generalized pressure, $p$ )
Boundary conditions at the solid liquid interface, $z=0$	no slip	$u=0$
	impermeable wall	$w=0$
	wall temperature	$\Theta=1$
Liquid-vapor interface jump conditions, $z=h(x,t)$ ,	Normal stress balance	$-Sj^2 + Cp = -h_{xx}(1 - F\Theta^I)$
	Shear stress balance	$\frac{C\theta_0^2}{F}u_z = -(\Theta_x + \Theta_z h_x)$
	Linearized energy balance	$N\Theta^I = -\Theta_z$
	Mass balance	$EN\Theta^I = w - h_t - uh_x$
Constitutive relation for mass flux: $j = N\Theta^I$		
Dimensionless numbers		
$N = \left( \frac{L\theta_o\alpha\rho_v H_l^2}{\lambda_l T_s^{3/2}} \right) \left( \frac{M}{2\pi R_g} \right)^{1/2}$	$C = \left( \frac{\eta_l U_o}{\sigma_s \theta_o^3} \right)$	
$F = \left( \frac{\gamma\Delta T}{\sigma_s} \right)$	$S = \left( \frac{\lambda_l \Delta T}{L\theta_o H_l} \right)^2 \left( \frac{L}{\sigma_s \rho_v \theta_o} \right)$	
$E = \left( \frac{\lambda_l \Delta T}{\rho_l H_l L U_o \theta_o^2} \right)$	$\bar{A} = \frac{A}{6\pi\eta_l U_o L^2 \theta_o}$	

If there is no evaporation, or the system is isothermal, i.e.,  $\Delta T=0$ , then the interface  $h(x,t)$  behaves as if it is impermeable to matter,  $E=0$ , and the kinematic boundary condition reduces to its familiar form:

$$\frac{\partial h}{\partial t} = w - u \frac{\partial h}{\partial x}. \quad (77)$$

Table I summarizes the set of dimensionless balance equations (mass, momentum, and energy), and their related boundary conditions, in their final simplified form.

This concludes the formulation of the nonisothermal microscale model of the three-phase contact zone. The approach was based on hydrodynamics, heat transfer, surface tension, and intermolecular long-range forces. The theoretical model consists of a system of differential equations of mass, momentum, and energy conservation, and their boundary conditions. The second part of the four-part series describing the work [14] includes the derivation of the interface equation, emerging from this model, and also its solution, as a parametric study of the film thickness behavior and analysis of the related phenomena. Subsequent parts of this series [15,18] deal with the determination of the rewetting temperature and velocity, by applying additional considerations of thermodynamics and heat transfer.

### III. SUMMARY AND CONCLUSIONS

(1) The rewetting phenomena is usually treated as being a problem of heat and mass transfer, and its modeling is pro-

vided in macroscale geometry. Here the work is concerned with the formulation of a nonisothermal microscale,  $O(1000 \text{ \AA})$ , rewetting model. The microscale model is focused in a region defined in Ref. [20] as a ‘‘proximal region.’’ In this region, the intermolecular solid-liquid forces and the effect of contact angle must be accounted for in the momentum balance equation. The contact angle, which is typically very small in rewetting situations [ $O(1^\circ)$ ], determines the geometry as well as the scales of the problem.

(2) The nature of the rewetting system, and its small contact angle, facilitate, through the use of the well known ‘‘lubrication approximation,’’ considerable simplifications of the balances equations (mass, momentum, and energy). Boundary conditions were formulated, both on the solid wall and at the liquid-vapor interface. The force and energy balances determine the boundary conditions at the liquid-vapor interface (i.e., shear stress, normal stress, energy balances, and kinematic condition).

(3) The boundary conditions, as well as the balance equations, were subjected to a process known as one-sided simplification. This process results in decoupling of the dynamics of the liquid and vapor phases. The set of equations accounts for several physical phenomena at the quench front. This is reflected, for example, in the normal stress boundary condition, where a term is included to describe the kinetic energy of evaporated fluid particles at the interface.

(4) The dynamic behavior of the fluid, at and across the interface, affects the solutions of the thermal and hydrodynamic fields. This is due to the dependence of these solutions on the interface profile,  $h(x)$ . The kinetic energy effect,

where the film is pushed by the evaporating liquid toward the solid wall, is known as the “recoil effect.” In case of intensive evaporation, this effect can even cause film rupture.

(5) The microscale hydrodynamic model involves the thermo-capillary number  $C/F$  and the capillary number  $C$ . In this model,  $C/F$  expresses the effect of temperature on the surface tension forces. The occurrence of a temperature gradient along the interface, in rewetting situations, imposes a corresponding gradient of surface tension. This changes the interface profile and the contact angle. The capillary number  $C$  provides a measure for the relative effects due to viscous and capillary forces. In rewetting, a film that moves with a smaller quench velocity involves smaller viscosity forces relative to the surface tension forces. In these cases, the surface tension is more dominant and smaller values of contact angle may be obtained.

(6) The microscale hydrodynamic model reflects the strong effect of the solid-liquid interactions on the film profile, and on the attendant flow and thermal fields. Thinner films, or alternatively smaller contact angles, are associated with stronger attraction forces between the solid and the liquid molecules. Consequently, rewetting can be established at higher temperatures of the solid surface. These attraction

forces also act against the tendency of the liquid to evaporate.

(7) The evaporation and conduction effects are incorporated in the dimensionless parameter  $S$ . Liquids with higher values of heat of evaporation  $H_l$ , are characterized by smaller values of  $S$ . In this case, the evaporation effect on the interface solution profile becomes less pronounced. The reverse is also true. The dimensionless parameter  $E$  is part of the kinematic boundary condition. This number also expresses the evaporation and conduction effects, but in contrast to  $S$ , which depends on the heat of evaporation, it relates to the kinematic behavior of the liquid-vapor interface. The case of interface that is impermeable to mass is obtained at  $E=0$ .

(8) The microscale nonisothermal hydrodynamic model, of the quench front forms the basis for analysis of the hydrodynamics involved in the rewetting phenomena. However, rewetting systems are also controlled by their thermodynamics, and, hence, the latter must be matched with the solution of the hydrodynamic model. This calls for the formulation of a combined hydrodynamic-thermodynamic model, for the description of rewetting phenomena, which is the subject of the subsequent parts of this series [14,15,18].

- 
- [1] V. Gerweck and G. Yadigaroglu, *Int. J. Heat Mass Transf.* **35**, 1823 (1992).
- [2] J. J. Carbajo and A. D. Siegel, *Nucl. Eng. Des.* **58**, 33 (1980).
- [3] M. Ben David, D.Sc. thesis, Technion—Israel Institute of Technology, Haifa, Israel, 1997.
- [4] P. J. Berenson, *J. Heat Transfer* **83**, 351 (1961).
- [5] R. E. Henry, in *Proceedings of the 14th National AMSE, AIChE Heat Transfer Conference, Atlanta, 1981*.
- [6] M. Shoji and N. Takagi, *Heat Transfer Jpn. Res.* **12**, 34 (1983).
- [7] R. E. Henry, *AIChE Symp. Ser.* **70**, 81 (1974).
- [8] H. Carslaw and J. Jaeger, *Conduction of Heat in Solids*, 2nd ed. (Clarendon, Oxford, 1959).
- [9] O. C. Iloge, W. M. Rohsenow, and P. Griffith, *J. Heat Transfer* **97**, 166 (1975).
- [10] M. De Salve and B. Panella, *Heat Technol.* **3**, 64 (1982).
- [11] P. Spiegler, J. Hopenfeld, M. Silbergberg, C. F. Bampus, and A. Norman, *Int. J. Heat Mass Transf.* **6**, 987 (1963).
- [12] K. J. Baumeister and F. F. Simon, *J. Heat Transfer* **94**, 166 (1973).
- [13] D. C. Wayner, Jr., *Int. J. Heat Mass Transf.* **22**, 1033 (1979).
- [14] M. Ben David, Y. Zimmels, and Y. Zvirin, *Determination of the Quench Velocity and Rewetting Temperature of Hot Surfaces: Analytical Solution of the Microscale Hydrodynamic Model*, *Int. J. Heat Mass Transf.* (to be published).
- [15] M. Ben David, Y. Zvirin, and Y. Zimmels, *Determination of the Quench Velocity and Rewetting Temperature of Hot Surfaces: A New Combined Hydrodynamic Thermodynamic Micro-scale Algorithm*, *Int. J. Heat Mass Transf.* (to be published).
- [16] D. E. Sullivan, *Phys. Rev. B* **20**, 3991 (1979).
- [17] D. E. Sullivan, *J. Chem. Phys.* **74**, 2604 (1981).
- [18] M. Ben David, Y. Zimmels, and Y. Zvirin, *Determination of the Quench Velocity and Rewetting Temperature of Hot Surfaces: A New Integrated Approach of Micro- and Macro-scale Models*, *Int. J. Heat Mass Transf.* (to be published).
- [19] S. Olek, Y. Zvirin, and E. Elias, *Int. J. Multiphase Flow* **14**, 13 (1988).
- [20] P. G. de Gennes, X. Hua, and P. Levinson, *J. Fluid Mech.* **212**, 55 (1990).
- [21] P. G. de Gennes, *Rev. Mod. Phys.* **57**, 827 (1985).
- [22] E. Ruckenstein and R. K. Jain, *J. Chem. Soc., Faraday Trans.* **70**, 132 (1974).
- [23] R. G. Owen and D. J. Pulling, in *Seminar on Underlying Programme: Fluid Phenomena Area Harwell, Oxfordshire, England, 1981*.
- [24] J. M. Delhay, *Int. J. Multiphase Flow* **1**, 395 (1974).
- [25] H. J. Palmer, *J. Fluid Mech.* **75**, 487 (1976).
- [26] J. P. Burelbach, S. G. Bankoff, and S. H. Davis, *J. Fluid Mech.* **195**, 463 (1988).
- [27] B. Spindler, J. N. Solesio, and J. M. Delhay, in *Chemical Process and Energy Engineering Systems*, edited by F. Durst, G. V. Tsikauri, and N. H. Afgan (Hemisphere, New York, 1978), Vol. 1, pp. 339–344.
- [28] P. Ehrhard and S. H. Davis, *J. Fluid Mech.* **229**, 365 (1991).
- [29] R. L. Hoffman, *J. Colloid Interface Sci.* **56**, 460 (1975).
- [30] L. H. Tanner, *J. Phys. D* **12**, 1473 (1979).